

Synthesis and characterization of submicron zirconia–12 mol% ceria ceramics

E.N.S. Muccillo*, D.M. Ávila

Instituto de Pesquisas Energéticas e Nucleares, Comissão Nacional de Energia Nuclear, C.P. 11049, S. Paulo, 05422-970, SP, Brazil

Received 15 January 1998; accepted 9 April 1998

Abstract

Zirconia powders containing 12 mol% ceria have been prepared by the coprecipitation technique. The aim of the present work was to obtain nanosized powders with suitable sinterability and reduced grain size in the sintered ceramic by means of this solution technique in its simplest route, that is, without using any milling or other special procedure. To accomplish those requests some processing variables have been systematically studied. For comparison purposes, specimens of the same composition have been prepared by the powder mixing technique. The optimization of some processing variables allowed for obtaining sintered specimens with apparent densities of 98% of the theoretical value, 100% of tetragonal phase, and 500 nm of average grain size. © 1999 Elsevier Science Limited and Techna S.r.l. All rights reserved.

Keywords: A. Powders: chemical preparation; B. Grain size; D. ZrO₂

1. Introduction

Over the past few years a growing interest has been observed on tetragonal zirconia polycrystals stabilized with Y₂O₃ (Y-TZP) or CeO₂ (Ce-TZP) mainly due to their improved thermomechanical properties. Ce-TZP shows high toughness, good thermal stability and low mechanical strength compared to Y-TZP [1]. One of the disadvantages of Ce-TZP is its low sinterability [2]. Moreover, its average grain size is comparatively larger than in Y-TZP [1] after similar processing conditions.

Different techniques have been used to prepare zirconia–ceria solid solutions: mixing of oxides [3], sol–gel [4,5], electrofusion [6], rapid solidification [7], and coprecipitation [8–13].

Simultaneous precipitation or coprecipitation is currently used to prepare zirconia-based ceramics in both laboratory scale and industrial scale, because it possesses many advantages over other processing techniques [14]. In comparison with conventional techniques, the coprecipitation technique produces nanosized powders usually with high sinterability and improved chemical homogeneity. In addition, the milling procedure is normally unnecessary, hence avoiding powder contamination. Besides its operational simplicity, the copre-

cipitation technique involves a number of variables that should be controlled for processing reproducibility. These processing variables influence the microstructure of the sintered ceramic thereby affecting their microstructure-related properties.

There are relatively few works dealing with the effect of optimization of these variables on the microstructure of the sintered ceramic. Some results in the literature indicate that the cation solution concentration governs the precipitate morphology. A reduction in the sintered density for increasing concentration of the cation solution was also observed [15]. The precipitant agent solution concentration has several effects on the precipitate. For Mg-doped zirconia it has been shown that it reduces the anion content in the gel, the crystallization temperature, and the initial temperature for the tetragonal to monoclinic martensite phase transformation [16]. In the case of solid solution synthesis, it is usual to perform the process by adding the cation solution to the precipitant solution. This procedure avoids segregation effects when the initial precipitation pH of the cations largely differs. The phase assemblage after calcination and the average crystal size are also defined by this variable. Less studied was the effect of precipitation temperature. It was recently shown [17] that for a fixed pH value there is an increase in the monoclinic phase fraction along with a reduction in the average crystal

* Corresponding author.

size with the increase of the precipitation temperature. One of the most studied processing variables is the washing medium because it controls the agglomeration state of the precipitate [18–21]. An additional step of washing with organic liquids is usually employed giving rise to a gel with soft agglomerates. Finally, the calcination of the dried powder must be scheduled in such a way that it allows for crystallization along with minor reduction in the value of the specific surface area. Although different processing conditions result in powders with some structural differences, many of these are lost during sintering [22]. However, to obtain improved microstructure in the sintered ceramics these processing variables should be studied and modified according to the type and concentration of the cations.

This solution technique has been successfully applied to other zirconia-based solid solutions. For the zirconia–ceria system, however, it should be emphasized that some complementary steps in the processing sequence are often necessary, in order to attain high densification and reduced grain size. Crystallization in organic solvents or water [11], and milling [8–10,12] or sieving [13] steps have been used for these purposes. Even though high sintered densities have been obtained, the average grain size was in the 1 to 3 μm range.

In this work some of these processing variables have been systematically studied in order to obtain nanosized zirconia–ceria powders with suitable sinterability and reduced grain size in the sintered ceramic by means of this solution technique in its simplest route. For comparison purposes, specimens of the same composition were prepared by the powder mixing technique.

2. Experimental procedure

2.1. Powder and specimens preparations

$\text{ZrOCl}_2 \cdot 8 \text{H}_2\text{O}$ (>99%, BDH) and $\text{Ce}(\text{NO}_3)_3 \cdot 6 \text{H}_2\text{O}$ (>99.5%, IPEN) were used as starting materials. The cerium nitrate solution was synthesized at IPEN starting from a rich-cerium (~85%) rare-earth concentrate by ion-exchange resin and fractionated precipitation techniques. Fig. 1 shows the experimental sequence for specimens prepared by the coprecipitation technique. The aqueous cation solution was added to a previously determined amount of precipitant solution under vigorous stirring. After precipitation completion, the system was kept under stirring for 2 h. The resultant gelatinous precipitate was washed (250 ml for each 50 ml of initial zirconyl chloride solution) and collected by vacuum filtration several times. The precipitant ammonia solution concentration was varied between 1 and 9 M. Most of these experiments have been done at room temperature (RT). In one experiment, however, the ammonia solution was held at 55°C during the coprecipitation step.

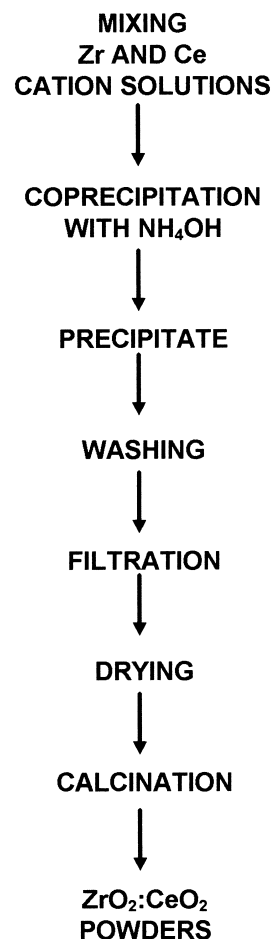


Fig. 1. Experimental sequence for synthesis by the coprecipitation technique.

Washing was performed in water or in a diluted ammonia solution and twice with ethanol after ultrasonic dispersion. The used reagents were of analytical grade. Calcination was carried out for 1 h at a temperature chosen after thermal analysis results. Other synthesis variables were fixed according to previous results. All experiments have been done at a fixed pH value of 10 by adding a 0.1 M cation solution at a rate of 50 ml min^{-1} to the ammonia solution. The precipitate was dried in air and at 45°C for 24 h. Nominal ceria concentration was 12 mol%. Cylindrical pellets have been prepared by uniaxial pressing at 98 MPa and cold isostatic pressing at 206 MPa. Sintering has been carried out at 1500°C for 2 h.

Specimens of the same nominal composition were prepared by the powder mixing technique. ZrO_2 (DK-1 type, Zirconia Sales) and CeO_2 (99.6%, IPEN) were mechanically mixed (Turbula model T2C) in ethanol using alumina as milling media. After drying at 45°C the powder was gently ground in an agate mortar. Pressing has been carried out in a similar way as for the coprecipitated powder. Sintering has been done in air at 1500°C for 1 h.

2.2. Characterizations

Powder analysis comprises: metallic impurity contents by inductively coupled plasma (ICP), chloride content by pyrohydrolysis, mass loss by thermogravimetric analysis (Du Pont model 951), particle distribution by sedimentation (Sedigraph model 5100, Micromeritics), and powder morphology by scanning electron microscopy, SEM (JXA 6400, Jeol; XL 30, Philips).

Sintered specimens characterizations have been carried out by X-ray diffractometry, XRD (Philips model 3710, X'Pert MPD) using a Ni filtered Cu K_{α} radiation. Lattice parameters have been calculated using Si as internal standard [23]. Phase content was estimated from the intensity ratio of the main monoclinic (m) and tetragonal (t) reflections [24]. Apparent densities have been determined by the water displacement method. Microstructural analysis has been done by SEM observations on polished and thermally etched surfaces of the specimens.

3. Results and discussion

3.1. Powder materials

Table 1 shows the metallic impurity contents determined by inductively coupled plasma in the precursor materials used to prepare zirconia–ceria both by coprecipitation and powder mixing techniques. High values of aluminum and magnesium were found in commercial zirconyl chloride whereas cerium nitrate presents a high silicon content. These chemical elements are known to be responsible for liquid phase sintering of this system, and secondary phase formation at grain boundaries [1].

Zirconyl chloride and cerium nitrate have been used for the coprecipitations. The basic experimental sequence is shown in Fig. 1. As it has already been stated, some of the processing variables were studied and optimized. One of them was the precipitation temperature. Fig. 2 shows SEM micrographs of powders coprecipitated at (a) room temperature and (b) 55°C, respectively, after calcination at 600°C. Besides porous and nearly spherical agglomerates of varying size some particles/agglomerates with flat surfaces and well defined

edges are also observed. The amount of these angular-shaped agglomerates is higher for the powder coprecipitated at 55°C.

The apparent densities of sintered cylindrical specimens prepared with these powders are quite different as shown in Table 2. The observed difference in density values suggests that the angular-shaped agglomerates are non-porous and tougher than the spherical agglomerates in such a way that they could not be broken during powder compaction. Other experiments carried out at precipitation temperatures lower than room temperature did not show improvement in the sintered density.

The above results are in disagreement with those obtained for the zirconia–magnesia system [22]. In the latter, increasing the precipitation temperature resulted in a relatively lower value of the average crystallite size and higher sintered density. It is well known that the mechanism of precipitate formation is governed by the rates of particle nucleation and growth. These results suggest that during the precipitation step the kinetic effects of the dopant cation particles play a major role in the mechanism of crystallite and particle growth of the calcined powder, thereby affecting grain growth during sintering.

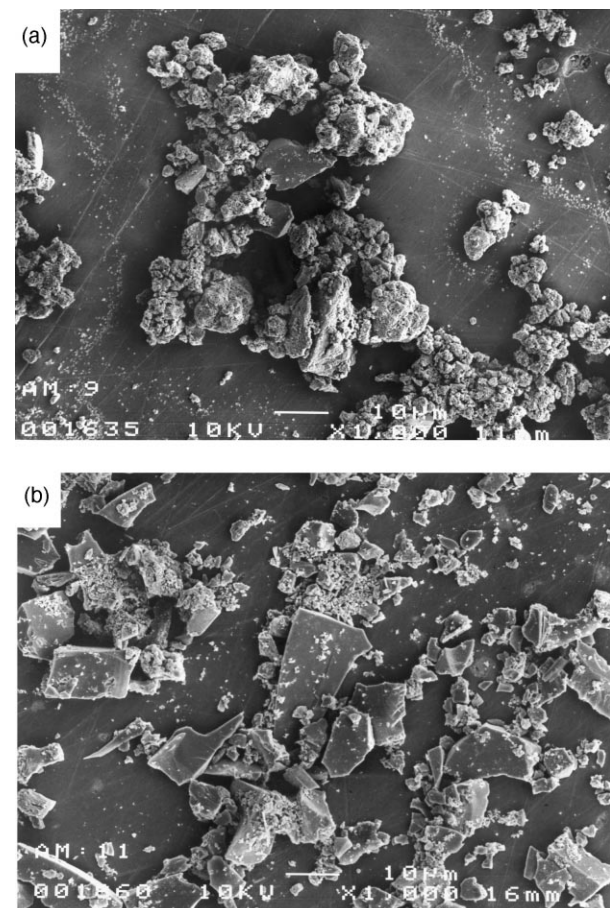


Fig. 2. SEM micrographs of powders coprecipitated at: (a) room temperature and (b) 55°C.

Table 1
Metallic impurity contents (in wt%) determined by ICP technique in raw materials

Elements	ZrOCl ₂ ·8H ₂ O	Ce(NO ₃) ₃ ·6H ₂ O	ZrO ₂	CeO ₂
Si	0.03	0.15	0.02	<0.006
Al	0.005	0.03	0.004	<0.006
Mg	>0.02	<0.0045	0.01	<0.0045
Ca	–	0.03	–	0.02

Table 2
Values of apparent density (d_h) determined by the hydrostatic method (in %T.D.) of sintered specimens prepared under different precipitation temperature and precipitant solution concentration

d_h (%T.D.)	Precipitation temperature	Precipitant solution concentration (M)
72	55°C	1
89	RT	1
83	RT	3
71	RT	6
76	RT	9

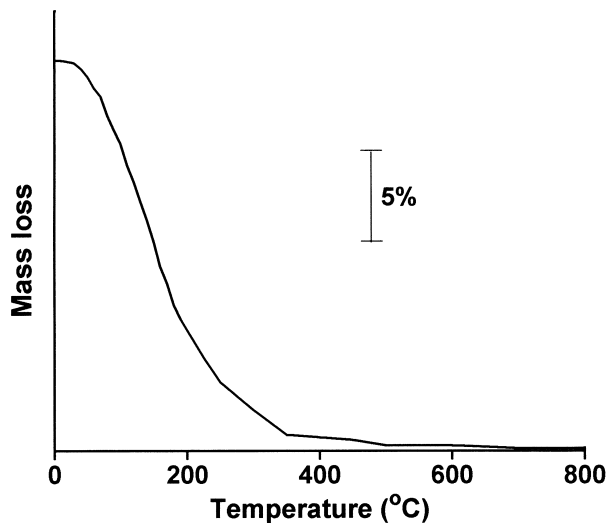


Fig. 3. Thermogravimetric curve of dried coprecipitated powder.

The effect produced by the precipitant solution concentration in the sintered density is shown in Table 2. Increasing the ammonia solution concentration decreases the sintered density. Recently [25] a similar effect was observed for yttria-doped ceria ceramics prepared by the oxalate coprecipitation method.

Several washing cycles have been tried. A combination of six times washing with a diluted (10 vol%) ammonia followed by twice with absolute ethanol has resulted in finely dispersed powders. The chloride content was 35 ppm as determined by pyrohydrolysis.

The calcination temperature of 600°C was chosen from thermogravimetric results. Fig. 3 is a typical TG curve. The mass loss up to 600°C is about 21% and beyond this temperature it is negligible, in good agreement with previous results [17].

For these optimized parameters, the morphology of the calcined powder is shown in the SEM micrograph in Fig. 4. Particles/agglomerates are relatively large reaching more than 20 μm in their largest dimension. These particles/agglomerates have low mechanical strength resulting in high density sintered specimens. The green density was only 37% of the theoretical value, and increased to 45 and 61% after subsequent thermal

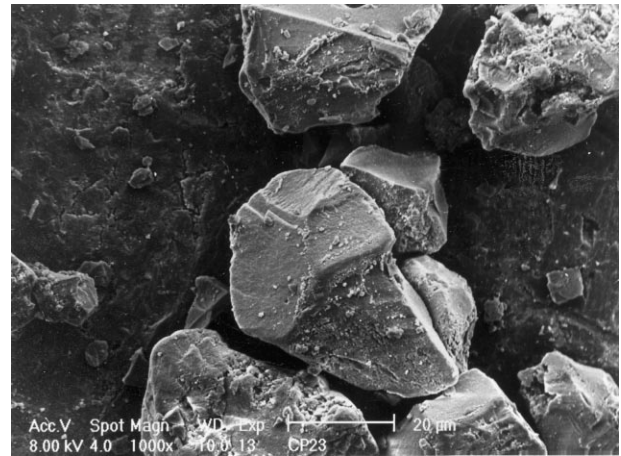


Fig. 4. SEM micrograph of the calcined powder.

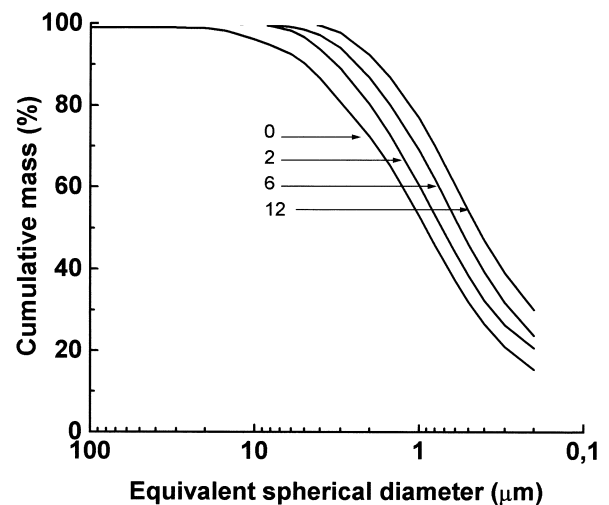


Fig. 5. Particle size distribution of powders prepared by mixing of oxides by different mixing times.

treatments at 800 and 1000°C, respectively. This means that improving some of the processing variables, a very reactive powder that starts to sinter at low temperatures can be obtained.

For comparison purposes, ZrO_2 and CeO_2 have been used to prepare specimens with the same nominal composition by the powder mixing technique. Table 1 shows the content of the main impurities found in these oxides. The most important impurity, in this case, is silicon at a level normally found in commercial zirconia powders.

Fig. 5 shows particle size distributions after mixing for 2, 6 and 12 h. The “0” curve was obtained for a powder after mixture in an agate mortar for 5 min. The average particle/agglomerate sizes determined at 50% cumulative mass are 0.92, 0.73, 0.56 and 0.44 μm for “0”, 2, 6 and 12 h of mixing, respectively. From these results, an ideal time of 6 h for mixing was chosen. This mixing step was important because of the different morphology of the starting oxide powders. Fig. 6 shows

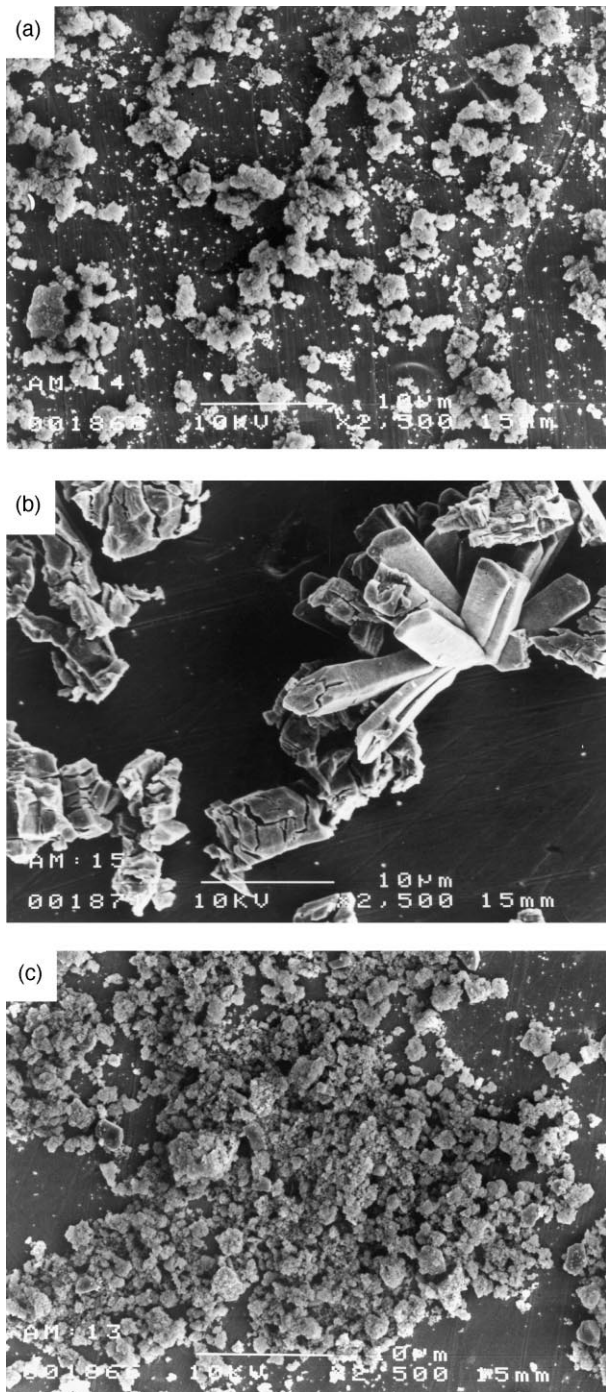


Fig. 6. SEM micrographs of (a) ZrO₂ (DK-2), (b) CeO₂ and (c) zirconia–ceria after 6 h of mixing.

Table 3
Tetragonal phase fraction (%), lattice parameters (in nm) and hydrostatic density (% T.D.) for sintered specimens

Technique	Tetragonal phase (%)	Lattice parameters (nm)		d_h (%T.D.)
		a	c	
Powder mixing	100	0.513(0)	0.523(0)	92
Coprecipitation	100	0.513(1)	0.525(8)	98

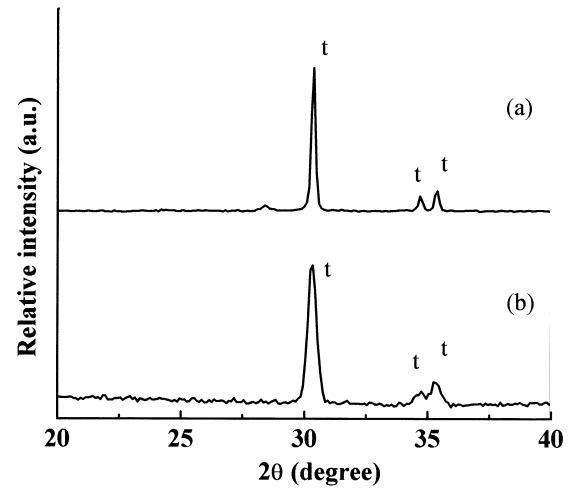


Fig. 7. XRD patterns of sintered specimens prepared by: (a) mixing of oxides and (b) coprecipitation techniques.

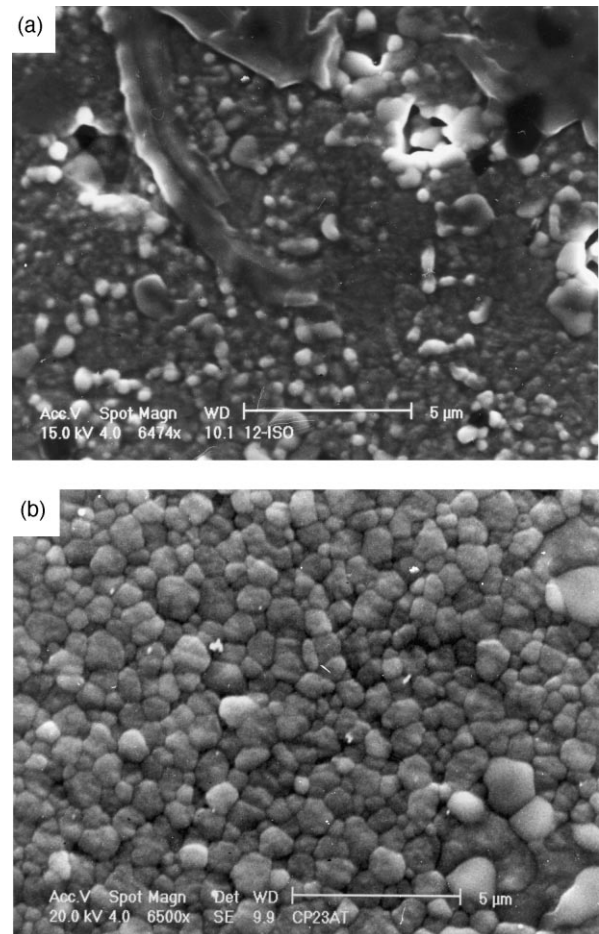


Fig. 8. SEM micrographs of sintered specimens prepared by: (a) mixing of oxides and (b) coprecipitation techniques.

SEM micrographs of (a) ZrO₂, (b) CeO₂ and (c) powders mixed for 6 h. After pressing, the green density reached 50% of the theoretical value.

3.2. Sintered specimens

From these optimized parameters, cylindrical specimens have been prepared by uniaxial and cold isostatic pressing. Sintering was carried out at a temperature (1500°C) lower than that where oxygen loss from CeO₂ was observed to occur resulting in decreased sintered density [10].

X-ray diffraction patterns for sintered specimens are shown in Fig. 7. They exhibit only the main reflections of the tetragonal phase. This shows that total stabilization of the tetragonal phase has been achieved for this composition independent on the technique employed for sample preparation. Lattice parameters determined using Si as internal standard are shown in Table 3. These figures are in good agreement with results obtained earlier for the same ceria concentration [8]. The calculated theoretical density (T.D.) value is 6.29 g cm⁻³.

Values of sintered density determined by the hydrostatic method are shown in Table 3. For specimens prepared with mixed powders, a maximum value of 92% T.D. was obtained. Specimens prepared with coprecipitated powders reached 98% T.D. without using any comminution process or other special step during processing. This result is ascribed to the optimization of the synthesis parameters.

Fig. 8 shows typical micrographs of thermally etched surfaces for specimens prepared by the two processing techniques. Specimens prepared with mixed powders exhibit non-uniform distribution of grain sizes with an estimated average value of 2 μm (Fig. 8a), normally found in zirconia–ceria ceramics. Secondary phases are also present, in this case, and are a consequence of powder contamination with the milling media during processing. Energy dispersive analysis shows that these phases contain aluminum, silicon and calcium as the major elements. In contrast, for specimens prepared with coprecipitated powders, relative low porosity and uniform grain size are the main microstructural features (Fig. 8b). From the grain size distribution an average value of 500 nm was determined.

4. Summary

In this work, two processing techniques have been used to prepare zirconia–12 mol% ceria ceramics. By means of the conventional powder mixing technique, sintered ceramics with 92% T.D., 100% of tetragonal phase, and an average grain size of 2 μm have been obtained. This system is known by its low sinterability and high grain size in comparison with other zirconia-based materials [1,2]. Some previous experiments using the coprecipitation technique [8–13] have resulted in high values of sintered density (≥98% T.D.). However,

the grain size was always in the 1 to 3 μm range. In order to know to what extent the variables involved in the coprecipitation technique influence the sinterability and grain growth in this system, some of these variables were studied and optimized. It was found that the washing medium and the way it is performed, the precipitation temperature, and the precipitant solution concentration are the most important parameters, in this case. Sintered ceramics prepared with coprecipitated powders reached 98% T.D., were fully tetragonal and had an average grain size of ~500 nm. The most important fact is that this synthesis technique was carried out in its simplest way, that is, without any further comminution or other special step. The main results show that this solution technique can be greatly improved whenever the influence of the processing variables are taken into account.

Acknowledgements

The authors are grateful to CNEN and FINEP for financial support, to Zirconia Sales for providing the ZrO₂ sample, and to A.C.S. Queiroz, K.F. Portella, S. Silva and C.V. Morais for technical assistance.

References

- [1] J.D. Cawley, W.E. Lee, in: R.W. Cahn, P. Haasen, E.J. Kramer (Eds.), *Materials Science and Technology, a Comprehensive Treatment*, in: M.V. Swain (Ed.), *Structure and Properties of Ceramics*, Vol. 11, VCH, Weinheim, Germany, 1994, pp. 47–117.
- [2] J.-H. Park, S.-W. Moon, Stability and sinterability of tetragonal zirconia polycrystals costabilized by CeO₂ and various oxides, *J. Mater. Sci. Lett.* 11 (1992) 1046–1048.
- [3] J.S. Wang, J.F. Tsai, D.K. Shetty, A.V. Virkar, Effect of MnO on the microstructures, phase stability, and mechanical properties of ceria partially-stabilized zirconia (Ce–TZP) and Ce–TZP–Al₂O₃ composites, *J. Mater. Res.* 5 (1990) 1948–1957.
- [4] S. Meriani, Thermal evolution of ceria–zirconia metallorganic precursors, *Thermochim. Acta* 58 (1982) 253–259.
- [5] V.S. Nagarajan, K.J. Rao, Characterization of sol–gel derived zirconia with additions of yttria and ceria. Origin of high fracture toughness in ceria-stabilized samples, *Phil. Mag.* A65 (1992) 778–781.
- [6] J. Wang, C.B. Ponton, P.M. Marquis, The grain boundary modification of ceria-stabilized tetragonal zirconia polycrystals by a small amount of alumina addition, *J. Mater. Sci. Lett.* 12 (1993) 702–705.
- [7] S. Torng, K. Miyazawa, T. Sakuma, The diffusionless cubic-to-tetragonal phase transition in near-stoichiometric ZrO₂–CeO₂, *Ceram. Int.* 22 (1996) 309–315.
- [8] J.-G. Duh, H.-T. Dai, W.-Y. Hsu, Synthesis and sintering behaviour in CeO₂–ZrO₂ ceramics, *J. Mater. Sci.* 23 (1988) 2786–2791.
- [9] J.-G. Duh, H.-T. Dai, Sintering, microstructure, hardness, and fracture toughness behavior of Y₂O₃–CeO₂–ZrO₂, *J. Am. Ceram. Soc.* 71 (1988) 813–819.
- [10] P. Duran, M. Gonzalez, J.R. Jurado, C. Moure, in: G.L. Messing, S.I. Hirano, H. Hausner (Eds.), *Ceramic Powder Science III*, *Ceramic Transactions*, Vol. 12, American Ceramic Society, Westerville, OH, 1990, pp. 945–952.

- [11] T. Sato, K. Dosaka, T. Yoshioka, A. Okuwaki, K. Torii, Y. Onodera, Sintering of ceria-doped tetragonal zirconia crystallized in organic solvents, water, and air, *J. Am. Ceram. Soc.* 75 (1992) 552–556.
- [12] S. El. Houe, Proceedings First International Spring School and Symposium on Advances in Materials Science, Vol. 2, 15–20 March 1994, Cairo, Egypt, pp. 535–547.
- [13] S. Maschio, A. Trovarelli, Powder preparation and sintering behaviour of ZrO_2 -20 mol% CeO_2 solid solutions prepared by various methods, *Br. Ceram. Trans.* 94 (1995) 191–195.
- [14] D.W. Johnson, in: G.L. Messing, K.S. Mazdiyasi, J.W. McCauley, R.A. Haber (Eds.), *Ceramic Powder Science, Advances in Ceramics*, Vol. 21, American Ceramic Society, Westerville, OH, 1987, pp. 3–19.
- [15] D.R. Spink, J.H. Schemel, The development of rare-earth pyrohafnates for power reactor control-rod material, *J. Nucl. Mater.* 49 (1973) 1–9.
- [16] T.Y. Tseng, C.C. Lin, J.T. Liaw, Phase transformations of gel-derived magnesia partially stabilized zirconias, *J. Mater. Sci.* 22 (1987) 965–972.
- [17] D.M. Ávila, E.N.S. Muccillo, Influence of some variables of the precipitation process on the structural characteristics of fine zirconia powders, *Thermochim. Acta* 256 (1995) 391–398.
- [18] M.A.C.G. van de Graaf, K. Keizer, A.J. Burggraaf, Influence of agglomerates in ultra-fine substituted zirconia powders on compaction and sintering behavior, *Sci. Ceram.* 10 (1979) 83–92.
- [19] F.F. Lange, Sinterability of agglomerated powders, *J. Am. Ceram. Soc.* 67 (1984) 83–89.
- [20] J.-L. Shi, J.-H. Gao, T.-S. Yen, Sintering behavior of fully agglomerated zirconia compacts, *J. Am. Ceram. Soc.* 74 (1991) 994–997.
- [21] J.L. Shi, Z.X. Gao, Z.-X. Lin, D.S. Yan, Effects of agglomerates in ZrO_2 powder compacts on microstructural development, *J. Mater. Sci.* 28 (1993) 342–348.
- [22] D.M. Ávila, E.N.S. Muccillo, Effects of synthesis parameters on electrical conductivity and microstructural development of fine zirconia powders, *J. Mater. Sci. Lett.* 16 (1997) 685–688.
- [23] H. Toraya, Effect of $YO_{1.5}$ on unit-cell parameters of ZrO_2 at low contents of $YO_{1.5}$, *J. Am. Ceram. Soc.* 72 (1989) 662–664.
- [24] R.C. Garvie, P.S. Nicholson, Phase analysis in zirconia systems, *J. Am. Ceram. Soc.* 55 (1972) 303–305.
- [25] J. van Herle, T. Horita, T. Kawada, N. Sakai, H. Yokokawa, M. Dokiya, Fabrication and sintering of fine yttria-doped ceria powders, *J. Am. Ceram. Soc.* 80 (1997) 933–940.